ARTICLE
Journal of Cellular Biochemistry 109:196–204 (2010)

Journal of Cellular Biochemistry

Hypoxia-Inducible Factors 1α and 2α Exert Both Distinct and Overlapping Functions in Long Bone Development

Stacy H. Shomento,[1] Chao Wan,[2] Xuemei Cao,[3] Marie-Claude Faugere,[4] Mary L. Bouxsein,[5] Thomas L. Clemens,[2] and Ryan C. Riddle[2]*

[1]*Department of Obstetrics and Gynecology, University of Alabama at Birmingham, Birmingham, Alabama*
[2]*Department of Orthopaedic Surgery, Johns Hopkins University School of Medicine, Baltimore, Maryland*
[3]*Department of Pathology, University of Alabama at Birmingham, Birmingham, Alabama*
[4]*Department of Medicine, University of Kentucky, Lexington, Kentucky*
[5]*Department of Orthopaedic Surgery, Beth Israel Deaconess Medical Center, Boston, Massachusetts*

ABSTRACT

The hypoxia-inducible factors have recently been identified as critical regulators of angiogenic–osteogenic coupling. Mice overexpressing HIFα subunits in osteoblasts produce abundant VEGF and develop extremely dense, highly vascularized long bones. In this study, we investigated the individual contributions of Hif-1α and Hif-2α in angiogenesis and osteogenesis by individually disrupting each Hifα gene in osteoblasts using the Cre-loxP method. Mice lacking *Hif-1α* demonstrated markedly decreased trabecular bone volume, reduced bone formation rate, and altered cortical bone architecture. By contrast, mice lacking *Hif-2α* had only a modest decrease in trabecular bone volume. Interestingly, long bone blood vessel development measured by angiography was decreased by a similar degree in both ΔHif-1α and ΔHif-2α mice suggesting a common role for these Hifα subunits in skeletal angiogenesis. In agreement with this idea, osteoblasts lacking either *Hif-1α* or *Hif-2α* had profound reductions in VEGF mRNA expression but only the loss of Hif-1α impaired osteoblast proliferation. These findings indicate that expression of both Hif-1α and Hif-2α by osteoblasts is required for long bone development. We propose that both Hif-1α and Hif-2α function through cell non-autonomous modes to promote vascularization of bone and that Hif-1α also promotes bone formation by exerting direct actions on the osteoblast. J. Cell. Biochem. 109: 196–204, 2010.

KEY WORDS: HYPOXIA-INDUCIBLE FACTOR; OSTEOBLAST; ANGIOGENESIS; SKELETAL DEVELOPMENT

The mammalian skeleton is formed through the concerted actions of its principle cell types, osteoblasts and osteoclasts, and requires the interaction of bone cells with skeletal vascular elements. During endochondral bone formation, blood vessels invade the cartilaginous model of developing long bones and deliver osteo-progenitors or osteogenic cues that result in the formation of the primary ossification center and the mineralization of skeletal tissue [Kronenberg, 2003; Provot and Schipani, 2005]. Genetic or pharmacological approaches to manipulate this interaction impair bone mineralization and reduce bone strength [Trueta and Amato, 1960; Zelzer et al., 2002]. During adult bone remodeling, blood vessels also interact with and influence the activities of resident osteoblasts and osteoclasts [Hauge et al., 2001; Eriksen et al., 2007]. Bone lining cells that express mediators of osteoclastogenesis seal off the bone remodeling compartment from the adjacent marrow, while an associated blood vessel serves as a conduit for circulating progenitor cells.

The molecular mechanisms responsible for angiogenic–osteogenic coupling are not well understood, but recent evidence suggests that hypoxia-inducible factors (Hifs) are key mediators of this interaction. Members of the Per-ARNT-Sim subfamily of basic helix-loop-helix transcription factors, the activity of Hifs are regulated by an oxygen-sensitive proteolytic mechanism [Wang et al., 1995]. At oxygen tensions above 5%, the α-subunit of Hif is hydroxylated by one of three oxygen-sensitive prolyl hydroxylase domain containing proteins [Bruick and McKnight, 2001] and recognized by the von Hippel–Lindau (Vhl) tumor suppressor protein, a component of the E3 ubiquitin ligase complex that targets Hifα for degradation [Ivan et al., 2001; Jaakkola et al., 2001]. Under hypoxic conditions, prolyl hydroxylation is inhibited. As a result

Grant sponsor: NIH; Grant number: AR049410.
*Correspondence to: Dr. Ryan C. Riddle, PhD, Department of Orthopaedic Surgery, Johns Hopkins University School of Medicine, 601 N. Caroline Street, Baltimore, MD 21287. E-mail: rriddle1@jhmi.edu
Received 28 September 2009; Accepted 1 October 2009 • DOI 10.1002/jcb.22396 • © 2009 Wiley-Liss, Inc.
Published online 6 November 2009 in Wiley InterScience (www.interscience.wiley.com).

Hifα subunits accumulate, translocate to the nucleus and interact with the constitutively expressed Hif-1β subunit at hypoxia-response elements. Additionally, a number of growth-factor signaling pathways provide a component of oxygen-independent regulation for Hif activity [Zelzer et al., 1998; Akeno et al., 2002; Semenza, 2002] by enhancing the synthesis of Hifα [Laughner et al., 2001] or by phosphorylating Hifα and thereby increasing its transcriptional activity [Richard et al., 1999; Land and Tee, 2007].

Two α subunits, Hif-1α and Hif-2α, which may have arisen by gene duplication [Iyer et al., 1998b], activate overlapping and distinct sets of target genes [Hu et al., 2003, 2006] involved in angiogenesis, cell proliferation, and metabolism. A third subunit, Hif-3α, appears to function as an inhibitor of Hif-1α function [Makino et al., 2007]. We have previously shown that osteoblasts express both Hif-1α and Hif-2α and that overexpression through the disruption of *Vhl* results in a striking and progressive increase in bone volume and a corresponding increase in skeletal vascularity [Wang et al., 2007]. Since this genetic manipulation results in the overexpression of both Hif-1α and Hif-2α, the individual roles of these transcription factors in skeletal development are unclear.

To distinguish the roles of Hif-1α and Hif-2α, we used a genetic approach to selectively disrupt each gene in osteoblasts. We demonstrate that both Hif-1α and Hif-2α are required for normal bone acquisition, but function via divergent mechanisms. Our results suggest that both Hif-1α and Hif-2α function through cell non-autonomous modes to promote vascularization of bone but that Hif-1α also promotes bone formation via direct actions on the osteoblast.

MATERIALS AND METHODS

GENERATION OF HIF-1α AND HIF-2α CONDITIONAL KNOCKOUT MICE

Mice lacking *Hif-1α* in osteoblasts (ΔHif-1α) were previously described [Wang et al., 2007]. Hif-2α conditional knockout mice (ΔHif-2α) were generated by crossing osteocalcin-Cre mice [Zhang et al., 2002] with homozygous conditional mutants containing modified *Hif-2α* alleles (with *loxP* sites flanking exon 2) [Gruber et al., 2007] to generate OC-Cre $^{TG/-}$; *Hif-2α*$^{flox/-}$ mice. An additional cross with *Hif-2α*$^{flox/flox}$ mice generated OC-Cre $^{TG/-}$; *Hif-2α*$^{flox/flox}$ mice that were used for subsequent breeding. PCR of DNA isolated from ear biopsies was used to confirm genotypes. The University of Alabama at Birmingham Institutional Animal Care and Use Committee approved all procedures involving mice.

SKELETAL PHENOTYPING AND HISTOLOGICAL ANALYSIS

A desktop microCT (μCT40; SCANCO Medical) was used to obtain high-resolution images of the femur. The intact right femur of 6-week-old control, ΔHif-1α and ΔHif-2α mice was scanned at 45 keV with an isotropic voxel size of 6 μM. Scanning of trabecular bone was initiated at the mid-epiphysis and extended proximally for 3.6 mm (600 μCT slices), while cortical bone was assessed at the mid-diaphysis. Dynamic bone formation rate was measured by injection of two sequential 0.25 ml doses of calcein (0.8 mg/ml) delivered 3 and 8 days prior to sacrifice. The left femur was fixed in ethanol, dehydrated and embedded in methylmethacrylate. Three micron sections were cut with a Microm microtome and stained with modified Mason–Goldner trichrome stain. The numbers of osteoblasts and osteoclasts per bone perimeter were measured at standardized sites under the growth plate at a magnification of 200× using a semi-automatic method (Osteoplan II, Kontron). These parameters comply with the guidelines of the nomenclature committee of the American Society of Bone and Mineral Research [Parfitt et al., 1987].

ANGIOGRAPHY

Skeletal vascularity was assessed using a μCT-based angiography technique [Duvall et al., 2004]. Briefly, animals were euthanized, the thoracic cavity was opened, and the inferior vena cava was severed. The vasculature was flushed with 0.9% normal saline containing heparin (100 U/ml) at a pressure of approximately 100 mmHg via a needle inserted into the left ventricle. Specimens were fixed via perfusion with 10% neutral-buffered formalin, flushed with heparinized saline, and then perfused with a radiopaque silicone compound containing lead chromate (Microfil MC-122; Flow Tech). Samples were stored at 4°C overnight to allow polymerization of the contrast agent. Femurs were dissected from the specimens and fixed in 10% neutral-buffered formalin for 2 days before being decalcified for 72 h in Cal-Ex II (Fisher Scientific), a formic acid-based solution. Images were obtained using a high-resolution (16 μM isotropic voxel size) microCT imaging system and used to calculate vessel number and volume.

PRIMARY OSTEOBLAST ISOLATION AND ADENOVIRUS INFECTION

Osteoblasts were isolated from calvaria of newborn *Hif-1α*$^{flox/flox}$ and *Hif-2α*$^{flox/flox}$ mice by serial digestion in a 1.8 mg/ml collagenase type I (Worthington Biochemical) solution. Calvaria were digested in 10 ml of digestion solution for 15 min at 37°C with constant agitation. The digestion solution was then collected and the digest repeated an additional four times. Digestion solutions 3–5, which contain osteoblasts, were pooled and cultured in α-MEM containing 10% FBS and 1% penicillin/streptomycin at 37°C in a humidified incubator supplied with 5% CO_2. To disrupt Hif-1α and Hif-2α in vitro, osteoblasts were grown to approximately 70% confluence and then infected with control adenovirus expressing green-fluorescent protein (ad-GFP) or adenovirus expressing Cre recombinase (ad-Cre, Vector Biolabs) at an MOI of 100. Osteoblasts were harvested 48 h after adenoviral infection and deletion efficiency was assessed in a portion of the cell population by real-time PCR. The remaining cells were re-plated in 6-well plates for proliferation and differentiation assays.

OSTEOBLAST PROLIFERATION AND DIFFERENTIATION

Osteoblast proliferation was assessed by flow cytometry. Briefly, control, ΔHif-1α, and ΔHif-2α osteoblasts were plated in 6-well plates at 5,000 cells/cm^2 and cultured in α-MEM containing 1% FBS for 48 h. BrdU (10 μM) was added to the medium for the last 24 h before harvesting the cells. The cells were stained with anti-BrdU-APC and 7-amino-actinomycin D and analyzed by FACSCalibur (BD Biosciences). Twenty thousand events were collected for each

sample, and the results were analyzed with WinMDI version 2.8. For differentiation experiments, control, ΔHif-1α, and ΔHif-2α osteoblasts were grown to confluence in 6-well plates and then cultured for 14 days in differentiation media consisting of α-MEM, 10% FBS, 1% penicillin/streptomycin, 10 mM β-glycerol phosphate, and 50 μg/ml ascorbic acid. Fixed cells were stained with 1-Step NBT/BCIP (Pierce) to examine alkaline phosphatase expression. Mineralization was assessed via the von Kossa method in which fixed cells were exposed to UV light in the presence of 3% silver nitrate ($AgNO_3$).

QUANTITATIVE REAL-TIME PCR

Total RNA was extracted from osteoblasts using the Trizol method (Invitrogen). One microgram of pure RNA, as assessed spectrophotometrically using the A260/A280 ratio, was reverse transcribed using the iScript cDNA synthesis system (Bio-Rad). Two microliters of cDNA was then subjected to PCR amplification using iQ SYBR Green Supermix (Bio-Rad) and sequence-specific primer pairs in an Opticon Continuous Fluorescent Detector (MJ Research). Primer pairs consisted of the following: *Hif1α*, 5′-CAAGATCTCGGCGAAGCAA-3′ and 5′-GGTGAGCCTCATAACAGAAGCTTT-3′; *Hif2α*, 5′-CAACCTGCAGCCTCAGTGTATC-3′ and 5′-CACCACGTCGTTCTTCTCGAT-3′; *Vegf*, 5′-CCACGTCAGAGAGCAACATCA-3′ and 5′-TCATTCTCTCTATGTGCTGGCTTT-3′; *Runx2*, 5′-ATGCTTCATTCGCCTCAC-3′ and 5′-CTCACGTCGCTCATCTTG-3′; *Osterix*, 5′-ATGGCGTCCTCTCTGCTTG-3′ and 5′-TGAAAGGTCAGCGTATGGCTT-3′; *OC*, 5′-TCTGCTCACTCTGCTGAC-3′ and 5′-GGAGCTGCTGTGACATCC-3′; *β-actin*, 5′-CCCAGAGCAAGAGAGG-3′ and 5′-GTCCAGACGCAGGATG-3′. PCR reactions were performed in duplicate for each cDNA, averaged, and normalized to endogenous β-actin reference transcript.

STATISTICAL ANALYSIS

Results are expressed as mean ± SEM. All statistical tests were two-sided. A *P*-value less that 0.05 was considered significant. Comparability of two groups of data was assessed using a Student's *t*-test.

RESULTS

DECREASED BONE VOLUME IN MICE LACKING HIF-1α OR HIF-2α IN OSTEOBLASTS

To distinguish the individual functions of Hif-1α and Hif-2α in skeletal development, we analyzed the skeletal phenotype of mice selectively lacking either *Hif-1α* or *Hif-2α* in osteoblasts. Mice expressing the Cre recombinase driven by an osteocalcin promoter [Zhang et al., 2002] were crossed with mice homozygous for either a loxP-flanked *Hif-1α* allele [Ryan et al., 2000; Schipani et al., 2001] or a loxP-flanked *Hif-2α* allele [Gruber et al., 2007] (hereafter designated as controls) to obtain mice lacking either *Hif-1α* or *Hif-2α* in osteoblasts (hereafter designated as ΔHif-1α and ΔHif-2α, respectively). ΔHif-1α and ΔHif-2α mice were born at the expected mendelian ratios and were similar in size and weight to their respective control littermates.

Analysis of trabecular bone at the distal femur of 6-week-old mice by microCT revealed a decreased bone volume in the ΔHif-1α mice but not in the ΔHif-2α mutants (not shown). Quantitative histomorphometric analysis of 6-week-old ΔHif-1α mice at this site showed that bone formation rate was reduced by 58% compared to control (Fig. 1A,B, Table I). This was accompanied by a reduction in bone volume per tissue volume (52%, Fig. 1C) and an increase (78%) in trabecular spacing (Fig. 1D). Surprisingly, osteoblast numbers were slightly elevated in ΔHif-1α mice (Fig. 1E) in the face of a

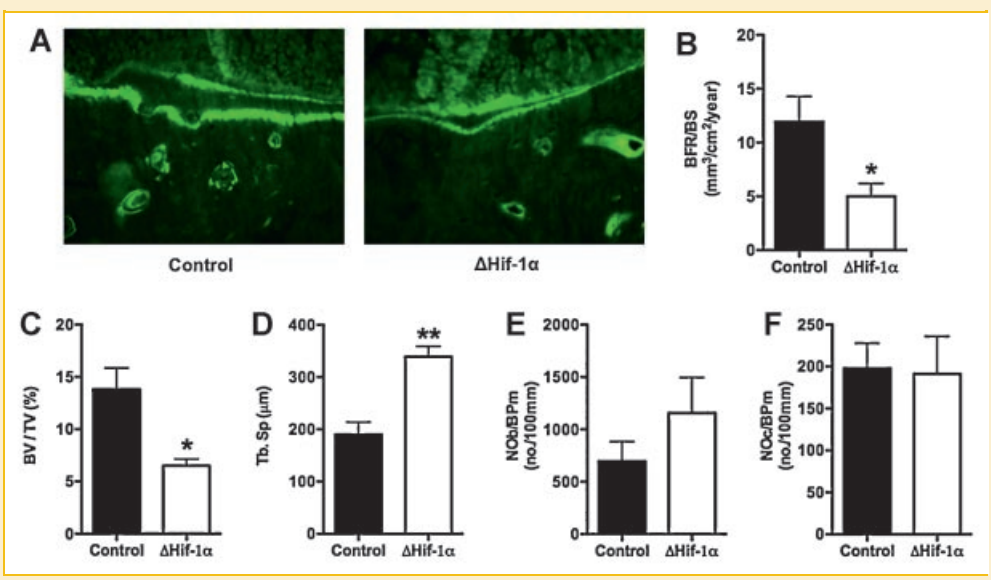

Fig. 1. Decreased bone volume in ΔHif-1α mice. Indices of skeletal structure and bone formation were assessed in the epiphyseal trabeculae of 6-week-old control and ΔHif-1α mice. Representative double calcein-labeled histological sections from control and ΔHif-1α mice are shown in A (40× original magnification). Histomorphometric measures of bone formation rate/bone surface (BFR/BS, B), bone volume/tissue volume (BV/TV, C), trabecular spacing (Tb.Sp, D), osteoblast number/bone perimeter (NOb/BPm, E), and osteoclast number/bone perimeter (NOc/BPm, F) are shown for control and ΔHif-1α mice (n = 4/genotype). $^{*}P < 0.05$; $^{**}P < 0.01$. [Color figure can be viewed in the online issue, which is available at www.interscience.wiley.com.]

TABLE I. Bone Histomorphometry

Bone parameter[a]	Control	ΔHif-1α	Control	ΔHif-2α
Bone structure				
Bone volume/tissue volume (BV/TV; %)	13.8 ± 2.02	6.51 ± 0.64[b]	16.1 ± 2.92	11.4 ± 0.94
Trabecular thickness (Tb.Th; μm)	29.9 ± 4.90	23.4 ± 1.96	30.8 ± 2.07	26.6 ± 2.39
Trabecular spacing (Tb.Sp; μm)	189 ± 23.9	339 ± 19.7[c]	171 ± 24.2	207 ± 10.6
Bone formation				
Osteoid volume/bone volume (OV/BV; %)	3.22 ± 0.71	1.95 ± 0.60	2.18 ± 0.82	2.24 ± 0.48
Osteoid surface/bone surface (OS/BS; %)	17.5 ± 2.34	13.6 ± 2.00	11.3 ± 2.89	14.1 ± 3.64
Osteoid thickness (O.Th; μm)	2.57 ± 0.46	1.54 ± 0.17	2.62 ± 0.33	2.17 ± 0.33
Osteoblast surface/bone surface (Ob.S/BS; %)	5.78 ± 1.54	9.13 ± 3.07	4.36 ± 1.54	6.89 ± 3.02
Osteoblast number/bone perimeter (NOb/BPm; no./100 mm)	696 ± 187	1156 ± 340	470 ± 214	754 ± 340.3
Bone erosion				
Erosion surface/bone surface (ES/BS; %)	5.12 ± 0.88	5.01 ± 1.33	2.88 ± 0.68	3.68 ± 0.81
Osteoclast surface (Oc.S/BS; %)	4.40 ± 0.65	4.05 ± 1.46	2.64 ± 0.63	2.84 ± 0.61
Osteoclast number/bone perimeter (NOc/BPm; no./100 mm)	198 ± 30.1	191 ± 44.9	106 ± 29.1	126 ± 30.0
Bone dynamics				
Mineral apposition rate (MAR; μm/day)	2.11 ± 0.24	1.51 ± 0.07[b]	1.73 ± 0.28	1.37 ± 0.17
Mineralizing surface/bone surface (MS/BS; %)	15.2 ± 1.56	8.62 ± 1.86[b]	10.3 ± 2.62	10.9 ± 2.49
Bone formation rate/bone surface (BFR/BS; $mm^3/cm^2/yr$)	11.9 ± 2.35	4.99 ± 1.20[b]	6.46 ± 1.55	5.86 ± 1.87
Mineralization lag time (Mlt; day)	1.90 ± 0.63	2.17 ± 0	2.15 ± 0.39	4.34 ± 2.20

[a]Values are shown as mean ± SE (n = 4 per genotype at 6 weeks of age).
[b]$P < 0.05$.
[c]$P < 0.01$.

reduced bone formation rate likely indicating a reduction in function of individual osteoblasts. Osteoclast numbers were not affected by the disruption of *Hif-1α* (Fig. 1F) suggesting that the decrease in bone volume was mainly due to decreased bone formation. In contrast to the histological changes seen in the ΔHif-1α mice, we observed only very modest effects on histomorphometric indices in the ΔHif-2α mice and these changes did not reach statistical significance (Table I). As an example, bone volume per tissue volume was decreased by 29% and bone formation rate was decreased by only 10% in ΔHif-2α mice when compared to controls.

Examination of the mid-shaft of the femur by microCT revealed disturbances in cortical bone architecture of 6-week-old ΔHif-1α mice, in agreement with our previous findings in 3-week-old mice [Wang et al., 2007]. Cross-sectional area of ΔHif-1α bones was significantly reduced compared to control (Fig. 2A,B) and the

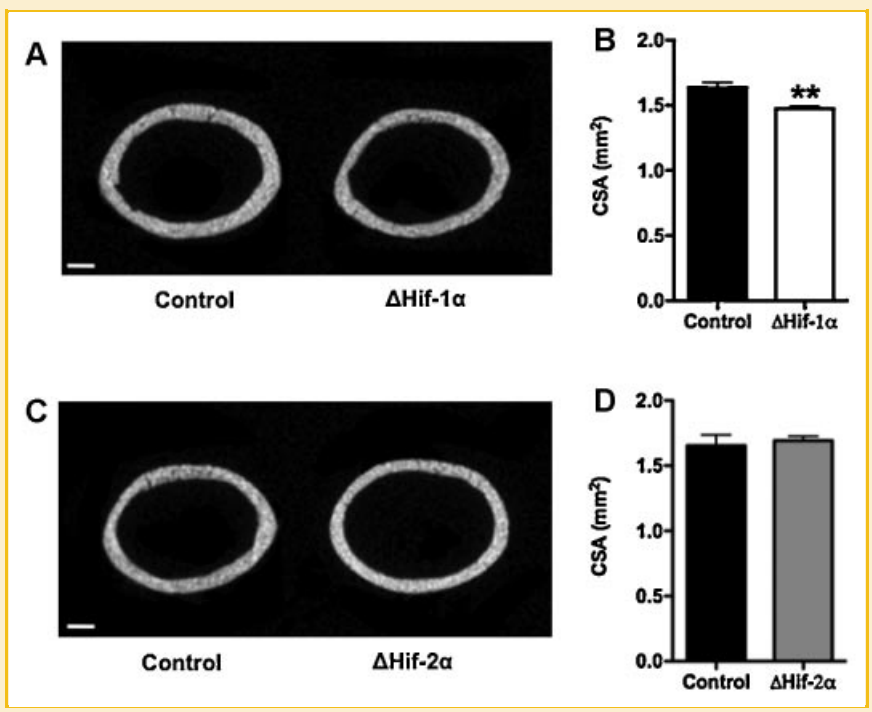

Fig. 2. Decreased cortical cross-sectional area in ΔHif-1α mice. μCT was utilized to examine cortical bone structure in 6-week-old mice. Representative images from the mid-diaphysis are shown for ΔHif-1α (A) and ΔHif-2α (C) mice as well as control littermates. Cross-sectional area is quantified for both genotypes (B and D, n = 4/genotype). $^{**}P < 0.01$.

cortices of the mutants tended to be thinner. In contrast, there was no noticeable effect of disrupting the expression of *Hif-2α* on cortical bone structure (Fig. 2C,D). Taken together these data indicate that Hif-1α subunit is required for normal trabecular and cortical bone accumulation whereas Hif-2α has a more limited role in these processes.

DECREASED SKELETAL VASCULARITY IN ΔHIF-1α AND ΔHIF-2α MICE

Since the induction of angiogenic factors including VEGF is a major function of both Hif-1α and Hif-2α, we next examined changes in skeletal vascularity in ΔHif-1α and ΔHif-2α mice. Mutant and control mice were perfused with Microfil and the skeletal vasculature was imaged by microCT (Fig. 3A,D). Quantitative analysis demonstrated that the disruption of *Hif-1α* resulted in a 41% decrease in vessel volume per tissue volume (Fig. 3B) and a 32% decrease in vessel number (Fig. 3C) when compared to controls. A similar impairment in the formation of vascular structures was evident in ΔHif-2α mice as vessel volume per tissue volume was decreased by 42% (Fig. 3E) and vessel number was decreased by 28% (Fig. 3F) compared to controls. Thus, both Hif-1α and Hif-2α are necessary for the normal development of the skeletal vasculature.

LOSS OF HIF-1α, BUT NOT HIF-2α, AFFECTS OSTEOBLAST FUNCTION IN VITRO

To determine whether Hifs might also influence skeletal development by exerting direct effects on osteoblasts, we examined the effect of disrupting *Hif-1α* or *Hif-2α* expression on osteoblast proliferation and differentiation in vitro. Calvarial osteoblasts were isolated from *Hif-1α*$^{flox/flox}$ mice and infected with Cre-expressing adenovirus or a GFP-expressing control. Ad-CRE infection resulted in a greater than 90% decrease in the expression of *Hif-1α* mRNA (Fig. 4A) and abolished the induction of *Vegf* mRNA in osteoblasts exposed to hypoxia (Fig. 4B). The loss of Hif-1α function was associated with impaired osteoblast proliferation, as BrdU incorporation was significantly decreased in ΔHif-1α osteoblasts when compared to controls (Fig. 4C). However, osteoblasts lacking *Hif-1α* differentiated normally; staining for alkaline phosphatase activity and mineralized nodule formation were comparable in control and ΔHif-1α osteoblasts after 14 days of culture in differentiation-inducing media (Fig. 4D). Similarly, the expression levels of runx2, osterix, and osteocalcin were similar in control and ΔHif-1α osteoblasts (data not shown). Ad-CRE infection decreased *Hif-2α* mRNA levels by more than 83% (Fig. 5A) and decreased *Vegf* mRNA levels by 52% after exposure to hypoxia (Fig. 5B). The loss of Hif-2α function, however, had no appreciable effect on osteoblast proliferation or differentiation, as levels of BrdU incorporation and staining for alkaline phosphatase activity and mineralized nodule

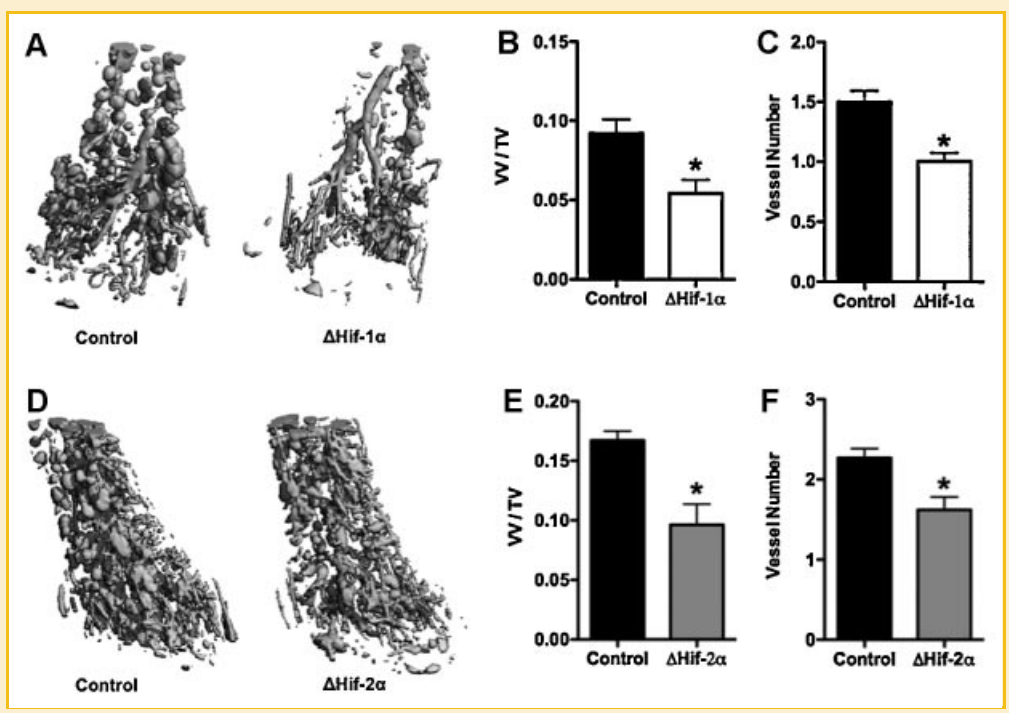

Fig. 3. Decreased angiogenesis in long bones of ΔHif-1α and ΔHif-2α mice. Control, ΔHif-1α, and ΔHif-2α mice (6-week old) were perfused with Microfil to assess skeletal vascularity in the distal femur. Representative μCT images of vascular structures are shown for ΔHif-1α (A) and ΔHif-2α (D) mice as well as for control littermates. Vessel volume and vessel number were quantified for control and ΔHif-1α mice (n = 3/genotype, B and C) and control and ΔHif-2α mice (n = 3/genotype, E and F). Scale bar = 200 μm. $^{*}P < 0.05$.

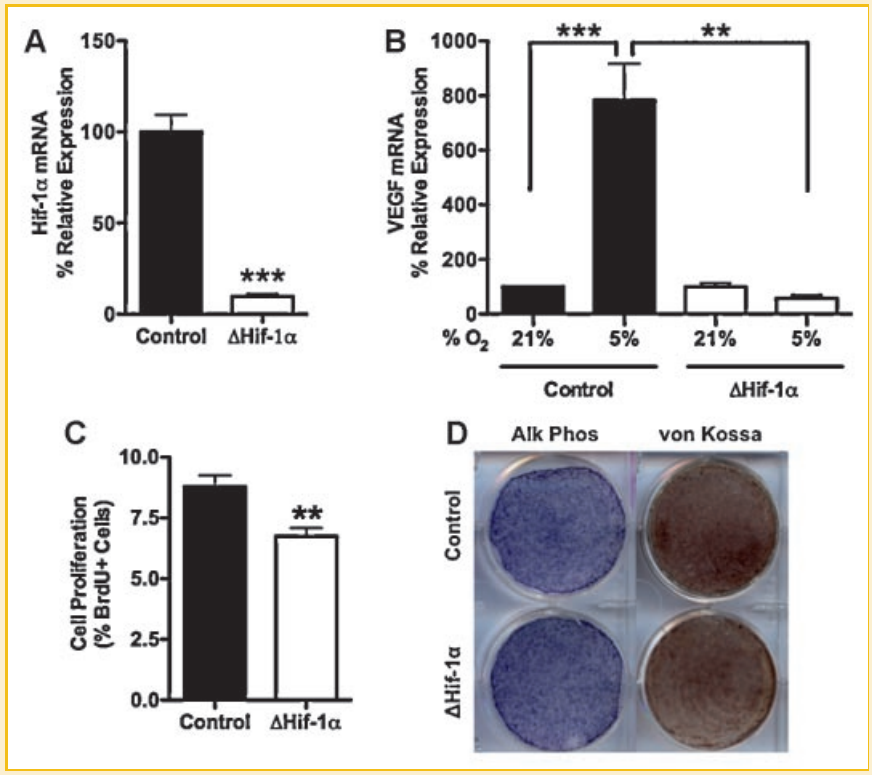

Fig. 4. Loss of Hif-1α impairs osteoblast proliferation but not differentiation. Calvarial osteoblasts were isolated from newborn Hif-1α$^{flox/flox}$ mice and infected with adGFP as control or adCRE to delete Hif-1α. After 2 days in culture, cells were analyzed for Hif-1α mRNA by real-time PCR (A). To assess Hif-1α function, control and ΔHif-1α osteoblasts were cultured under normoxic (21% O_2) or hypoxic (5% O_2) conditions and VEGF mRNA was examined by real-time PCR (B). Control and ΔHif-1α osteoblasts were serum-starved for 24 h and then cultured in the presence of BrdU for an additional 24 h. BrdU incorporation was quantified by FACS analysis as a marker of cellular proliferation (C). The effect of disrupting Hif-1α expression on osteoblast differentiation was assessed by staining control and ΔHif-1α osteoblasts for alkaline phosphatase and mineralization after 14 days of differentiation. $^{**}P < 0.01$; $^{***}P < 0.001$. [Color figure can be viewed in the online issue, which is available at www.interscience.wiley.com.]

formation were similar in control and ΔHif-2α osteoblasts (Fig. 5C,D). Likewise, the expression of runx2, osterix, and osteocalcin were unaffected by *Hif-2α* deletion (data not shown). Taken together, these data suggest that while Hif-1α exerts both cell-autonomous and -non-autonomous effects during skeletal development, Hif-2α serves only cell-non-autonomous functions.

DISCUSSION

Endochondral bone formation coincides both spatially and temporally with capillary in-growth and angiogenesis. If angiogenesis is experimentally disrupted, bone development is severely impaired [Coolbaugh, 1952; Trueta and Amato, 1960; Trueta and Buhr, 1963; Gerber et al., 1999]. The molecular mechanisms responsible for coupling angiogenesis and osteogenesis are not well understood, but recent work indicates that the hypoxia-inducible factor pathway plays a key role in orchestrating this interaction [Schipani et al., 2001; Wang et al., 2007]. Overexpressing Hifs in osteoblasts by selectively disrupting *Vhl* produces a striking and progressive increase in bone volume that is secondary to an increase in osteoblast number and activity. Since the deletion of *Vhl* produces no appreciable effect on osteoblast function in vitro and the increase in bone volume in vivo is accompanied by a marked increase in skeletal vascularity, the bone phenotype in these mice is most likely the result of Hif-mediated angiogenesis. However, the precise roles of individual Hifα subunits in this process remain unclear, and the extent to which Hifs exert direct effects on osteoblast function has not been explored.

Experiments designed to distinguish the functions of individual Hifα subunits in vivo are complicated by the fact that many cell types [Wiesener et al., 1998; Talks et al., 2000; Hu et al., 2003], including osteoblasts [Wang et al., 2007], express both Hif-1α and Hif-2α. Further, Hif-1α and Hif-2α are structurally similar, recognize the same DNA element, and dimerize with Hif-1β [Ema et al., 1997; Tian et al., 1997]. In order to investigate the individual contributions of these two related Hif subunits during skeletal development we used a genetic approach to disrupt selectively Hif-1α and Hif-2α in osteoblasts using Cre-mediated recombination.

Deletion of either HIF subunit was associated with defects in skeletal vascularity, reflected by reduced blood vessel number and volume. These data are consistent with the overlapping roles of Hifs in inducing angiogenesis. Both *Hif-1α*$^{-/-}$ mice and *Hif-2α*$^{-/-}$ mice exhibit embryonic lethality, which is at least partially attributable to blood vessel defects [Iyer et al., 1998a; Ryan et al., 1998; Peng et al., 2000], and each α subunit can induce the expression of *Vegf* [Hu et al., 2003, 2006]. Additionally, these observations agree with our previous results that suggested a role for both Hifα subunits in

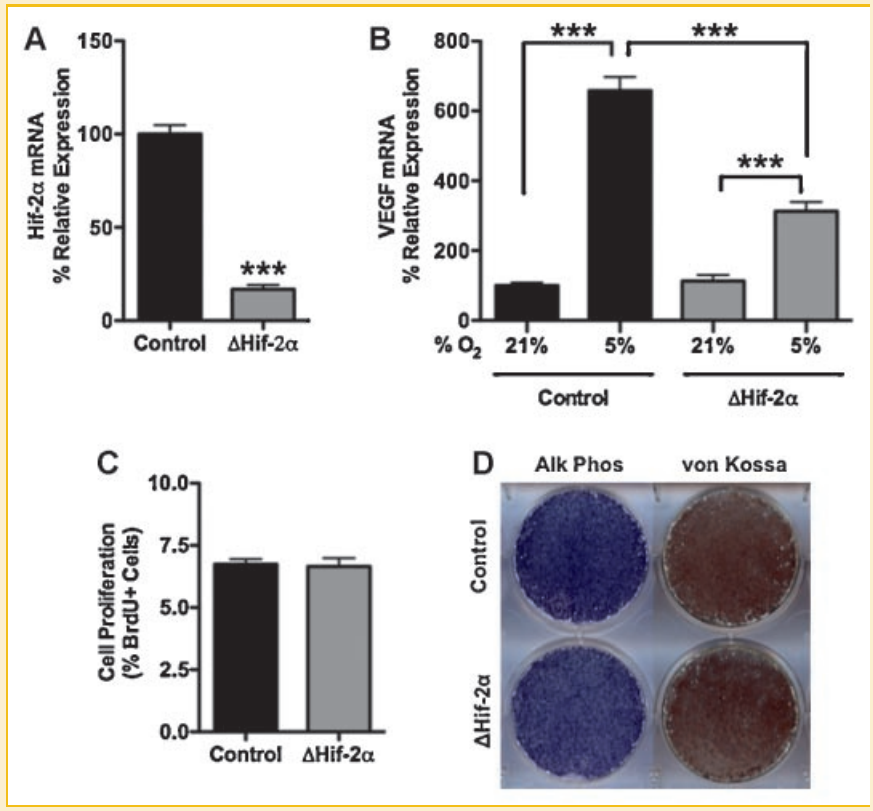

Fig. 5. Loss of Hif-2α does not impair osteoblast function. Calvarial osteoblasts were isolated from newborn Hif-2α$^{flox/flox}$ mice and infected with adGFP as control or adCRE to delete Hif-2α. Real-time PCR was used to quantify Hif-2α mRNA after adenoviral infection (A) as well as VEGF mRNA in control and ΔHif-2α osteoblasts after culture under normoxic (21% O_2) or hypoxic (5% O_2) conditions (B). Cellular proliferation was assessed in control and ΔHif-2α osteoblasts by culturing serum-starved cells in the presence of BrdU (C). Staining for alkaline phosphatase and mineralization were used to assess osteoblast differentiation (D). $^{**}P < 0.01$; $^{***}P < 0.001$. [Color figure can be viewed in the online issue, which is available at www.interscience.wiley.com.]

regulating skeletal vascularity. In that study, deletion of both *Hif-1α* and *Vhl* in osteoblasts, increased skeletal vascularity by a similar degree as that observed in bones from mice lacking only *Vhl* [Wang et al., 2007]. Since the targeted overexpression of stable forms of *Hif-1α* and *Hif-2α* phenocopies *Vhl* deletion in other tissues [Kim et al., 2006], these data suggested a role for Hif-2α as well as Hif-1α in regulating skeletal vascularity.

The fact that reductions in bone trabecular and cortical accumulation were more severe in ΔHif-1α mice clearly indicates that this subunit exerts additional actions distinct from those of Hif-2α in the osteoblast. For example, disruption of *Hif-1α* reduced osteoblast proliferation whereas disruption of *Hif-2α* did not. This finding is consistent with defects in proliferation observed in embryonic stem cells deficient in *Hif-1α* [Iyer et al., 1998a]. A role for Hif-1α in the proliferative behavior of mesenchymal cells could be explained by the proposed role of Hif-1α in the "Warburg" effect [Semenza, 2007]. During the proliferation process, cellular metabolism transitions from oxidative phosphorylation to aerobic glycolysis, perhaps in an attempt to accumulate the biomass necessary to produce a daughter cell [Vander Heiden et al., 2009] or to protect replicating DNA from damage induced by reactive oxygen species [Brand and Hermfisse, 1997]. In this regard, Hif-1α appears to be unique among Hifα subunits in the ability to increase the expression of glycolytic genes [Hu et al., 2003, 2006]. It is also plausible that the loss of Hif-1α function impairs proliferation by reducing expression of growth factors such as *Igf-2* [Feldser et al., 1999].

In spite of our in vitro findings that suggest Hif-1α is necessary for osteoblast proliferation, osteoblast numbers in 6-week-old ΔHif-1α mice were slightly elevated. It is possible that this is related to the use of the osteocalcin promoter to direct Cre expression. The osteocalcin promote should achieve its highest level of expression in mature osteoblasts [Zhang et al., 2002], and may not accurately replicate the in vitro experiments that utilized undifferentiated osteoblasts. However, it is also possible that the increase in osteoblasts numbers observed in vivo represents a compensatory mechanism engaged in response to impairments in osteoblast function. In support of this idea, we previously reported that osteoblast numbers are indeed decreased in 3-week-old ΔHif-1α mice [Wang et al., 2007].

Interestingly, the reduced accumulation of bone seen in the Hif-1α mutant mice occurred at all bone surfaces including the cortex. The influence of mechanical stimuli on cortical bone structure is well documented, and it is possible that Hif-1α plays a role in bone cell mechanotransduction. Hif-1α is upregulated following skeletal unloading as a result of osteocyte hypoxia [Gross et al., 2001], and by anabolic loading in other tissues. In the rat, hemodynamic loading of the heart or stretching cardiac tissue stimulates Hif-1α

accumulation [Kim et al., 2002], and similar observations have been made in stretched smooth muscle [Chang et al., 2003]. However, both Hifα subunits are reportedly upregulated by loading in muscle, where they play a role in angiogenesis [Milkiewicz et al., 2007]. Recent studies suggest that angiogenesis precedes load-induced bone formation [Yao et al., 2004; Matsuzaki et al., 2007], but a role for Hifs in this process has not yet been examined.

In summary, we established a model system to distinguish the roles of Hif-1α and Hif-2α in osteoblasts. Our results suggest that Hif-1α influences bone formation through cell autonomous mechanisms as well as cell non-autonomous mechanisms. By comparison, Hif-2α appears to only influence skeletal homeostasis by influencing angiogenesis. These results provide a broader understanding of the role of the hypoxia-inducible factor pathway during skeletal development.

ACKNOWLEDGMENTS

The authors thank Randall Johnson (University of California San Diego) and M. Celeste Simon (University of Pennsylvania) for generously supplying the Hif-1α floxed and Hif-2α floxed mice.

REFERENCES

Akeno N, Robins J, Zhang M, Czyzyk-Krzeska MF, Clemens TL. 2002. Induction of vascular endothelial growth factor by IGF-I in osteoblast-like cells is mediated by the PI3K signaling pathway through the hypoxia-inducible factor-2α. Endocrinology 143:420–425.

Brand KA, Hermfisse U. 1997. Aerobic glycolysis by proliferating cells: A protective strategy against reactive oxygen species. FASEB J 11:388–395.

Bruick RK, McKnight SL. 2001. A conserved family of prolyl-4-hydroxylases that modify HIF. Science 294:1337–1340.

Chang H, Shyu KG, Wang BW, Kuan P. 2003. Regulation of hypoxia-inducible factor-1α by cyclical mechanical stretch in rat vascular smooth muscle cells. Clin Sci (Lond) 105:447–456.

Coolbaugh CC. 1952. Effects of reduced blood supply on bone. Am J Physiol 169:26–33.

Duvall CL, Taylor WR, Weiss D, Guldberg RE. 2004. Quantitative micro-computed tomography analysis of collateral vessel development after ischemic injury. Am J Physiol Heart Circ Physiol 287:H302–H310.

Ema M, Taya S, Yokotani N, Sogawa K, Matsuda Y, Fujii-Kuriyama Y. 1997. A novel bHLH-PAS factor with close sequence similarity to hypoxia-inducible factor 1α regulates the VEGF expression and is potentially involved in lung and vascular development. Proc Natl Acad Sci USA 94:4273–4278.

Eriksen EF, Eghbali-Fatourechi GZ, Khosla S. 2007. Remodeling and vascular spaces in bone. J Bone Miner Res 22:1–6.

Feldser D, Agani F, Iyer NV, Pak B, Ferreira G, Semenza GL. 1999. Reciprocal positive regulation of hypoxia-inducible factor 1α and insulin-like growth factor 2. Cancer Res 59:3915–3918.

Gerber HP, Vu TH, Ryan AM, Kowalski J, Werb Z, Ferrara N. 1999. VEGF couples hypertrophic cartilage remodeling, ossification and angiogenesis during endochondral bone formation. Nat Med 5:623–628.

Gross TS, Akeno N, Clemens TL, Komarova S, Srinivasan S, Weimer DA, Mayorov S. 2001. Osteocytes upregulate HIF-1α in response to acute disuse and oxygen deprivation. J Appl Physiol 90:2514–2519.

Gruber M, Hu CJ, Johnson RS, Brown EJ, Keith B, Simon MC. 2007. Acute postnatal ablation of Hif-2α results in anemia. Proc Natl Acad Sci USA 104:2301–2306.

Hauge EM, Qvesel D, Eriksen EF, Mosekilde L, Melsen F. 2001. Cancellous bone remodeling occurs in specialized compartments lined by cells expressing osteoblastic markers. J Bone Miner Res 16:1575–1582.

Hu CJ, Iyer S, Sataur A, Covello KL, Chodosh LA, Simon MC. 2006. Differential regulation of the transcriptional activities of hypoxia-inducible factor 1 α (HIF-1α) and HIF-2α in stem cells. Mol Cell Biol 26:3514–3526.

Hu CJ, Wang LY, Chodosh LA, Keith B, Simon MC. 2003. Differential roles of hypoxia-inducible factor 1α (HIF-1α) and HIF-2α in hypoxic gene regulation. Mol Cell Biol 23:9361–9374.

Ivan M, Kondo K, Yang H, Kim W, Valiando J, Ohh M, Salic A, Asara JM, Lane WS, Kaelin WG, Jr. 2001. HIFα targeted for VHL-mediated destruction by proline hydroxylation: Implications for O2 sensing. Science 292:464–468.

Iyer NV, Kotch LE, Agani F, Leung SW, Laughner E, Wenger RH, Gassmann M, Gearhart JD, Lawler AM, Yu AY, Semenza GL. 1998a. Cellular and developmental control of O_2 homeostasis by hypoxia-inducible factor 1 α. Genes Dev 12:149–162.

Iyer NV, Leung SW, Semenza GL. 1998b. The human hypoxia-inducible factor 1α gene: HIF1A structure and evolutionary conservation. Genomics 52:159–165.

Jaakkola P, Mole DR, Tian YM, Wilson MI, Gielbert J, Gaskell SJ, Kriegsheim A, Hebestreit HF, Mukherji M, Schofield CJ, Maxwell PH, Pugh CW, Ratcliffe PJ. 2001. Targeting of HIF-α to the von Hippel-Lindau ubiquitylation complex by O_2-regulated prolyl hydroxylation. Science 292:468–472.

Kim CH, Cho YS, Chun YS, Park JW, Kim MS. 2002. Early expression of myocardial HIF-1α in response to mechanical stresses: Regulation by stretch-activated channels and the phosphatidylinositol 3-kinase signaling pathway. Circ Res 90:E25–E33.

Kim WY, Safran M, Buckley MR, Ebert BL, Glickman J, Bosenberg M, Regan M, Kaelin WG, Jr. 2006. Failure to prolyl hydroxylate hypoxia-inducible factor α phenocopies VHL inactivation in vivo. EMBO J 25:4650–4662.

Kronenberg HM. 2003. Developmental regulation of the growth plate. Nature 423:332–336.

Land SC, Tee AR. 2007. Hypoxia-inducible factor 1α is regulated by the mammalian target of rapamycin (mTOR) via an mTOR signaling motif. J Biol Chem 282:20534–20543.

Laughner E, Taghavi P, Chiles K, Mahon PC, Semenza GL. 2001. HER2 (neu) signaling increases the rate of hypoxia-inducible factor 1α (HIF-1α) synthesis: Novel mechanism for HIF-1-mediated vascular endothelial growth factor expression. Mol Cell Biol 21:3995–4004.

Makino Y, Uenishi R, Okamoto K, Isoe T, Hosono O, Tanaka H, Kanopka A, Poellinger L, Haneda M, Morimoto C. 2007. Transcriptional up-regulation of inhibitory PAS domain protein gene expression by hypoxia-inducible factor 1 (HIF-1): A negative feedback regulatory circuit in HIF-1-mediated signaling in hypoxic cells. J Biol Chem 282:14073–14082.

Matsuzaki H, Wohl GR, Novack DV, Lynch JA, Silva MJ. 2007. Damaging fatigue loading stimulates increases in periosteal vascularity at sites of bone formation in the rat ulna. Calcif Tissue Int 80:391–399.

Milkiewicz M, Doyle JL, Fudalewski T, Ispanovic E, Aghasi M, Haas TL. 2007. HIF-1α and HIF-2α play a central role in stretch-induced but not shear-stress-induced angiogenesis in rat skeletal muscle. J Physiol 583:753–766.

Parfitt AM, Drezner MK, Glorieux FH, Kanis JA, Malluche H, Meunier PJ, Ott SM, Recker RR. 1987. Bone histomorphometry: Standardization of nomenclature, symbols, and units. Report of the ASBMR Histomorphometry Nomenclature Committee. J Bone Miner Res 2:595–610.

Peng J, Zhang L, Drysdale L, Fong GH. 2000. The transcription factor EPAS-1/hypoxia-inducible factor 2α plays an important role in vascular remodeling. Proc Natl Acad Sci USA 97:8386–8391.

Provot S, Schipani E. 2005. Molecular mechanisms of endochondral bone development. Biochem Biophys Res Commun 328:658–665.

Richard DE, Berra E, Gothie E, Roux D, Pouyssegur J. 1999. p42/p44 mitogen-activated protein kinases phosphorylate hypoxia-inducible factor

1α (HIF-1α) and enhance the transcriptional activity of HIF-1. J Biol Chem 274:32631–32637.

Ryan HE, Lo J, Johnson RS. 1998. HIF-1 α is required for solid tumor formation and embryonic vascularization. EMBO J 17:3005–3015.

Ryan HE, Poloni M, McNulty W, Elson D, Gassmann M, Arbeit JM, Johnson RS. 2000. Hypoxia-inducible factor-1α is a positive factor in solid tumor growth. Cancer Res 60:4010–4015.

Schipani E, Ryan HE, Didrickson S, Kobayashi T, Knight M, Johnson RS. 2001. Hypoxia in cartilage: HIF-1α is essential for chondrocyte growth arrest and survival. Genes Dev 15:2865–2876.

Semenza G. 2002. Signal transduction to hypoxia-inducible factor 1. Biochem Pharmacol 64:993–998.

Semenza GL. 2007. HIF-1 mediates the Warburg effect in clear cell renal carcinoma. J Bioenerg Biomembr 39:231–234.

Talks KL, Turley H, Gatter KC, Maxwell PH, Pugh CW, Ratcliffe PJ, Harris AL. 2000. The expression and distribution of the hypoxia-inducible factors HIF-1α and HIF-2α in normal human tissues, cancers, and tumor-associated macrophages. Am J Pathol 157:411–421.

Tian H, McKnight SL, Russell DW. 1997. Endothelial PAS domain protein 1 (EPAS1), a transcription factor selectively expressed in endothelial cells. Genes Dev 11:72–82.

Trueta J, Amato VP. 1960. The vascular contribution to osteogenesis. III. Changes in the growth cartilage caused by experimentally induced ischaemia. J Bone Joint Surg Br 42-B:571–587.

Trueta J, Buhr AJ. 1963. The vascular contribution to osteogenesis. V. The vasculature supplying the epiphysial cartilage in rachitic rats. J Bone Joint Surg Br 45:572–581.

Vander Heiden MG, Cantley LC, Thompson CB. 2009. Understanding the Warburg effect: The metabolic requirements of cell proliferation. Science 324:1029–1033.

Wang GL, Jiang BH, Rue EA, Semenza GL. 1995. Hypoxia-inducible factor 1 is a basic-helix-loop-helix-PAS heterodimer regulated by cellular O_2 tension. Proc Natl Acad Sci USA 92:5510–5514.

Wang Y, Wan C, Deng L, Liu X, Cao X, Gilbert SR, Bouxsein ML, Faugere MC, Guldberg RE, Gerstenfeld LC, Haase VH, Johnson RS, Schipani E, Clemens TL. 2007. The hypoxia-inducible factor α pathway couples angiogenesis to osteogenesis during skeletal development. J Clin Invest 117:1616–1626.

Wiesener MS, Turley H, Allen WE, Willam C, Eckardt KU, Talks KL, Wood SM, Gatter KC, Harris AL, Pugh CW, Ratcliffe PJ, Maxwell PH. 1998. Induction of endothelial PAS domain protein-1 by hypoxia: Characterization and comparison with hypoxia-inducible factor-1α. Blood 92:2260–2268.

Yao Z, Lafage-Proust MH, Plouet J, Bloomfield S, Alexandre C, Vico L. 2004. Increase of both angiogenesis and bone mass in response to exercise depends on VEGF. J Bone Miner Res 19:1471–1480.

Zelzer E, Levy Y, Kahana C, Shilo BZ, Rubinstein M, Cohen B. 1998. Insulin induces transcription of target genes through the hypoxia-inducible factor HIF-1α/ARNT. EMBO J 17:5085–5094.

Zelzer E, McLean W, Ng YS, Fukai N, Reginato AM, Lovejoy S, D'Amore PA, Olsen BR. 2002. Skeletal defects in $VEGF_{120/120}$ mice reveal multiple roles for VEGF in skeletogenesis. Development 129:1893–1904.

Zhang M, Xuan S, Bouxsein ML, von Stechow D, Akeno N, Faugere MC, Malluche H, Zhao G, Rosen CJ, Efstratiadis A, Clemens TL. 2002. Osteoblast-specific knockout of the insulin-like growth factor (IGF) receptor gene reveals an essential role of IGF signaling in bone matrix mineralization. J Biol Chem 277:44005–44012.